Cx50 requires an intact PDZ-binding motif and ZO-1 for the formation of functional intercellular channels

Zhifang Chai[a], Daniel A. Goodenough[b], and David L. Paul[a]
[a]Department of Neurobiology and [b]Department of Cell Biology, Harvard Medical School, Boston, MA 02115

ABSTRACT The three connexins expressed in the ocular lens each contain PDZ domain–binding motifs directing a physical association with the scaffolding protein ZO-1, but the significance of the interaction is unknown. We found that Cx50 with PDZ-binding motif mutations did not form gap junction plaques or induce cell–cell communication in HeLa cells, whereas the addition of a seven–amino acid PDZ-binding motif restored normal function to Cx50 lacking its entire C-terminal cytoplasmic domain. C-Terminal deletion had a similar although weaker effect on Cx46 but little if any effect on targeting and function of Cx43. Furthermore, small interfering RNA knockdown of ZO-1 completely inhibited the formation of gap junctions by wild-type Cx50 in HeLa cells. Thus both a PDZ-binding motif and ZO-1 are necessary for Cx50 intercellular channel formation in HeLa cells. Knock-in mice expressing Cx50 with a PDZ-binding motif mutation phenocopied Cx50 knockouts. Furthermore, differentiating lens fibers in the knock-in displayed extensive intracellular Cx50, whereas plaques in mature fibers contained only Cx46. Thus normal Cx50 function in vivo also requires an intact PDZ domain–binding motif. This is the first demonstration of a connexin-specific requirement for a connexin-interacting protein in gap junction assembly.

INTRODUCTION

Gap junctions are clusters of intercellular channels that provide direct pathways for exchange of ions and small molecules between the cytoplasm of adjacent cells (Goodenough and Paul, 2009). Intercellular channels are composed of connexins, a 21-member family in humans. Gap junction assembly involves a number of steps that must be coordinated. Most connexins enter the classic secretory pathway involving transport from endoplasmic reticulum to Golgi complex, although some may also traffic in a Golgi-independent manner (Zhang *et al.*, 1996; Martin *et al.*, 2001; Qu *et al.*, 2009). During this process, connexin monomers oligomerize into hexamers, called connexons or hemichannels, generally required for delivery to the plasma membrane (Segretain and Falk, 2004; Koval, 2006; VanSlyke *et al.*, 2009). At the cell surface, apposing hemichannels interact to form intercellular channels and accrete into plaque-like or macular structures. The precise molecular mechanisms that underlie these sequential processes are not well understood.

One protein implicated in gap junction assembly is the membrane scaffolding protein ZO-1 (Stevenson *et al.*, 1986), which binds to a canonical motif at the C-termini of several connexins. Cx43 interacts with the second PDZ domain of ZO-1 (Giepmans and Moolenaar, 1998; Toyofuku *et al.*, 1998; Singh *et al.*, 2005), whereas Cx36 interacts with the first PDZ domains of ZO-1, ZO-2, and ZO-3 (Li *et al.*, 2004b, 2009; Flores *et al.*, 2008). In addition, it has been shown that Cx31.9 (Nielsen *et al.*, 2002), Cx45 (Kausalya *et al.*, 2001; Laing *et al.*, 2001), Cx47 (Li *et al.*, 2004a), and the lens fiber connexins Cx46 and Cx50 (Nielsen *et al.*, 2003) all bind directly to ZO-1.

Several studies suggest that ZO-1 binding may regulate gap junction assembly in a connexin- and cell type–specific manner. Truncation of Cx43 at residue 257 eliminated ZO-1 binding and caused myocardial gap junctions to become smaller and less organized in a knock-in mouse (Maass *et al.*, 2004). In contrast, blockade of the PDZ-binding motif in Cx43 by addition of a C-terminal green fluorescent protein (GFP) tag or administration of Cx43 C-terminal mimetic peptides led to a striking increase in gap junction area in HeLa cells and cultured wild-type (WT) myocardiocytes (Hunter *et al.*, 2005; Hunter and Gourdie, 2008). C-Terminal interactions also

Abbreviations used: FBS, fetal bovine serum; GFP, green fluorescent protein; HEPES, 4-(2-hydroxyethyl)-1-piperazineethanesulfonic acid; MW, molecular weight; PBS, phosphate-buffered saline; siRNA, small interfering RNA; WT, wild type.

influence the assembly of gap junctions containing Cx36, as transgenic expression of enhanced GFP-tagged Cx36 in Cx36-deficient mice failed to restore electrical coupling between interneurons (Helbig *et al.*, 2010). However, neither Cx43 nor Cx36 required a functional C-terminal PDZ-binding motif to efficiently form intercellular channels when expressed in paired *Xenopus* oocytes (Morley *et al.*, 1996; Helbig *et al.*, 2010). Cx50 also shows dependence on C-terminal sequences for normal function. Cx50 undergoes a natural cleavage in vivo at residue 290 (Lin *et al.*, 1997), which would be expected to eliminate ZO-1 binding. Although this truncation mutant induced junctional conductance in pairs of *Xenopus* oocytes (Lin *et al.*, 1998; Stergiopoulos *et al.*, 1999; Eckert, 2002; Derosa *et al.*, 2006) and in N2A cells (Xu *et al.*, 2002; Derosa *et al.*, 2006), it was less efficient than WT Cx50, consistent with the idea that ZO-1 binding could influence the assembly of Cx50 gap junctions. None of the truncations discussed materially affect single-channel conductances or voltage-gating properties, suggesting that the changes in connexin function reflect changes in some aspect of junction assembly. However, although these studies implicate ZO-1 in junction assembly, they do not demonstrate a requirement for ZO-1 or any other connexin-interacting protein.

In this study, we examined the relative importance of ZO-1 binding to Cx50, which, along with Cx46 and Cx43, constitutes a network of communication critical for maintaining optical transparency and regulating lenticular growth (White *et al.*, 1994, 1998). For Cx50, we found that deletion of the ultimate C-terminal residue eliminated the formation of junctional plaques and the induction of cell–cell communication in HeLa cells. C-terminal deletion had a similar although weaker effect on Cx46 but little if any effect on targeting and functioning of Cx43. Normal function was restored to Cx50 lacking most of its C-terminal cytoplasmic domain by the addition of seven C-terminal amino acids containing its PDZ-binding motif. In addition, knockdown of endogenous ZO-1 in HeLa cells by anti–human ZO-1 small interfering RNA (siRNA) treatment completely inhibited normal trafficking of WT Cx50 and development of cell–cell communication. Normal behavior was restored to WT Cx50 in ZO-1–depleted HeLa cells by transfection with mouse ZO-1, which was not affected by the anti–human ZO-1 siRNAs. Thus both a PDZ-binding motif and ZO-1 are necessary for Cx50 to form junctional plaques and active intercellular channels in HeLa cells. To explore the significance of the Cx50 PDZ-binding motif in vivo, we created knock-in mice expressing Cx50 lacking its ultimate C-terminal amino acid residue. Differentiating lens fibers in the knock-in displayed extensive intracellular Cx50, whereas plaques in mature fibers contained only Cx46. In addition, the anatomical phenotypes were very similar to Cx50-null mice. Thus normal Cx50 function in vivo also requires an intact PDZ domain–binding motif. This study provides the first demonstration of a connexin-specific requirement for a connexin-interacting protein in gap junction assembly. In addition, the difference in the requirement for ZO-1 by Cx43 and Cx50 implies multiple mechanisms for gap junction assembly.

RESULTS

Transfection of WT Cx50 into connexin-deficient, communication-incompetent HeLa cells (Magnotti *et al.*, 2011) produced strong punctate or macular immunofluorescence staining (Figure 1A), a pattern commonly observed with other connexins and indicative of gap junction formation. Some intracellular fluorescence signal, likely from Golgi and other intracellular membranes, was also evident, similar to that reported for Cx43 in NRK and S180L cells (Musil *et al.*, 1990). In contrast, deletion of the ultimate C-terminal isoleucine (Cx50Δ440) resulted in complete loss of macular localization

(Figure 1B). This result was robust and repeatable over several independent transfections (see *Materials and Methods*). Intracellular signal was increased compared with WT Cx50, and occasional diffuse staining at or near the plasma membrane (arrow) was observed. Western blotting revealed no obvious change in steady-state protein levels (unpublished data).

We assessed intercellular communication by microinjection of neurobiotin, a low–molecular mass (287 Da) tracer known to permeate gap junction channels comprised of most if not all connexins (Elfgang *et al.*, 1995; Manthey *et al.*, 2001; Orthmann-Murphy *et al.*, 2007). Because we used transient transfection, not all of the cells in each experiment were expected to express the connexin being tested. Therefore a fluorescent marker (Cerulean or Venus) was incorporated into the expression vector so that injections could be targeted to clusters of transfected cells. Marker expression was detected in a significant fraction of the cells (compare Figure 1, C and D, and Figure 1, F and G). After injection, cells were aldehyde fixed, and neurobiotin was detected with fluorescently labeled avidin. For WT Cx50 (Figure 1, C–E), the tracer was evident in a large number of cells surrounding the injected cell (Figure 1E, arrow) indicating a robust coupling by gap junctions. In contrast, Cx50Δ440 (Figure 1, F–H) induced no detectable dye coupling (Figure 1H), indicating that functional intercellular channels did not form. Similarly, expression of Cx50 with a C-terminal truncation at residue 420, 410, or 380 did not induce either the formation of junctional plaques or dye transfer (Figure 1, I–M), and expression of truncations at 350, 320, 300, or 290 did not induce dye transfer (Figure 1, N–Q). The subcellular distribution of deletions below 320 was not determined because the epitope recognized by our antibody was lost. Surprisingly, modest (~10% of WT) but highly reproducible dye coupling was induced by Cx50 truncated at residue 245, where the entire C-terminal cytoplasmic domain was eliminated (Figure 1R).

Wild-type Cx46, like Cx50, produced strong macular staining in HeLa cells (Figure 2A) and robust neurobiotin transfer (Figure 2B). Deletion of its ultimate C-terminal residue (Cx46Δ417) resulted in a major reduction but not complete loss of macular localization (Figure 2C) and a complementary reduction of dye transfer (Figure 2D). Truncation of Cx46 at residue 290 completely eliminated its ability to induce dye coupling in HeLa cells (Figure 2F), but, like Cx50, its subcellular distribution could not be directly assessed because the epitope recognized by our anti-Cx46 antibody was lost. To allow visualization of the mutants with deeper truncations, FLAG epitopes (Brizzard *et al.*, 1994) were added. Some intracellular and possible plasma membrane immunofluorescence signal was present, but plaque-like staining was never observed (Figure 2E). Wild-type Cx43 produced robust dye coupling (Figure 2G), which, as expected (Hunter *et al.*, 2005), was not affected by removal of either the ultimate C-terminal isoleucine (unpublished data) or of most of the C-terminal domain by truncation at residue 257 (Figure 2H).

The loss or reduction of function caused by single–amino acid deletions at the ultimate C-termini of Cx50 and Cx46 indicated that a critical determinant of normal trafficking lay close to the C-terminus. If it were the sole or major determinant, then its addition to an extensively truncated protein should restore functionality. Therefore we fused different lengths of C-terminal residues to Cx50 truncated at residue 290, expressed them in HeLa cells, and assessed dye coupling. Fusion constructs containing seven or more of the ultimate C-terminal residues induced coupling similar to WT Cx50, whereas constructs containing fewer than seven residues were completely nonfunctional (Figure 3, E–M). For some constructs, subcellular distribution was assessed by including FLAG epitopes, as we had for Cx46. Whereas Cx50Δ290-440+FLAG exhibited neither macular
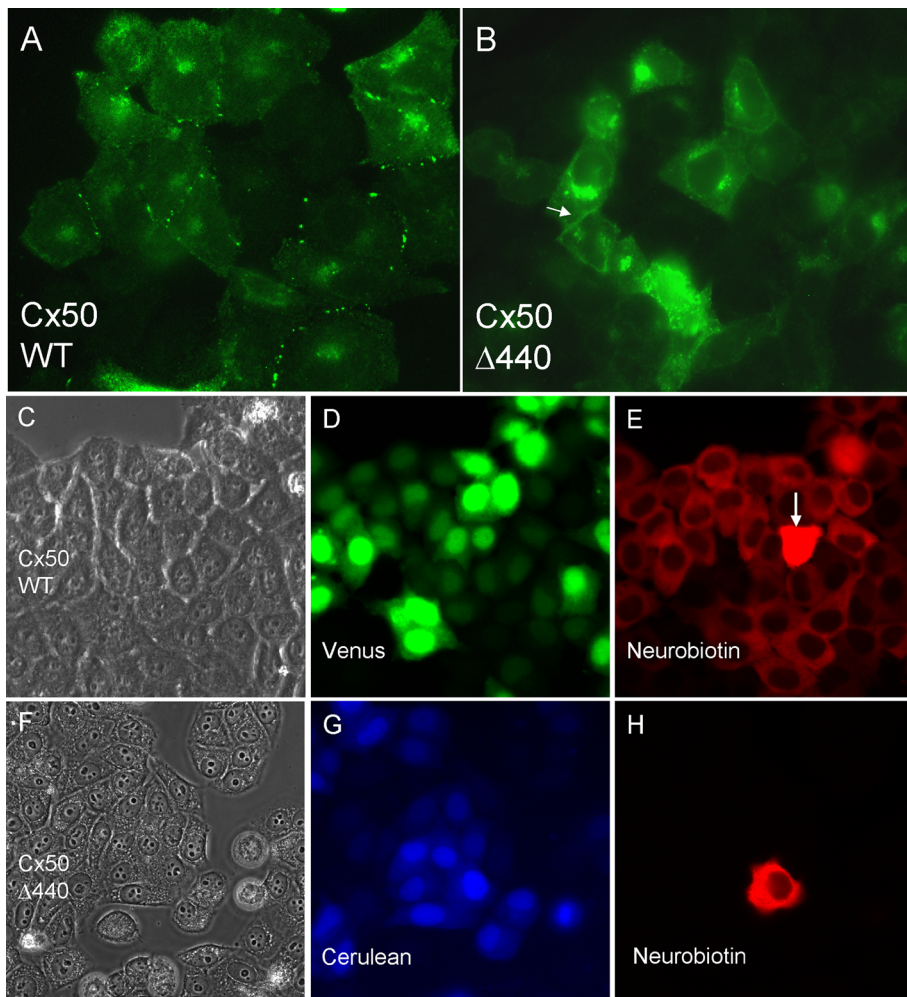
M1 E1 M2 M3 E2 M4 · Cx50 · C-terminus

	Cx50 C-terminus	Cells Coupled	Distribution
I	WT (440aa)	41.2±8.8	Plaques
J	Δ440	0.09±0.3	IM, PM
K	Δ421-440	0.08±0.3	IM, PM
L	Δ411-440	0.10±0.3	IM, PM
M	Δ381-440	0.10±0.3	IM, PM
N	Δ351-440	0.09±0.3	IM
O	Δ321-440	0.14±0.4	IM
P	Δ301-440	0.10±0.3	ND
Q	Δ291-440	0.07±0.02	ND
R	Δ246-440	4.3±3.1	ND

FIGURE 1: The ultimate C-terminal residue of Cx50 is required for efficient assembly of gap junctions and formation of active intercellular channels. (A) Transfection of wild-type Cx50 into connexin-deficient, communication-incompetent HeLa cells produced strong punctate immunofluorescence staining at cell–cell interfaces, a pattern commonly observed with other connexins and indicative of gap junction formation. Some intracellular signal, likely from Golgi and other intracellular membranes, was also evident. (B) In contrast, Cx50Δ440, which lacked only the ultimate C-terminal isoleucine, displayed no macular localization, increased intracellular staining, and occasional diffusely distributed signal at or near the plasma membrane (arrow). (C–H) Microinjection of neurobiotin was used to assess junctional coupling. A fluorescent marker (Cerulean or Venus) was incorporated into the expression vector so that injections could be targeted to clusters of transfected cells. For WT Cx50 (C–E), neurobiotin is evident in a large number of cells surrounding the injected cell (arrow), indicating robust coupling by gap junctions (E). In contrast, Cx50Δ440 (F–H) induced no detectable tracer coupling (H), indicating that functional intercellular channels did not form. More extensive truncations were similarly nonfunctional (I–Q), but a modest level of coupling was retained after nearly complete removal of the C-terminal cytoplasmic domain (R). E, extracellular domain; IM, intracellular membranes; M, membrane domain; ND, not determined; PM, plasma membrane.

localization nor conferred dye coupling (Figure 3, A, B, and N), the addition of the ultimate seven amino acids (Cx50Δ290-440+FLAG+RSDDLTI) was sufficient to restore normal behavior

(Figure 3, C, D, and O). Addition of RSDDLTI also restored WT levels of plaque formation and dye coupling to Cx50 truncated at residue 245 (Figure 3, P and Q). Identical results were obtained for Cx46Δ290-417+FLAG (Figure 2, E and F) and Cx46Δ290-417+FLAG+RPGDLAI (unpublished data). Together, these data show that the seven ultimate C-terminal amino acid residues are necessary and sufficient to direct the efficient assembly of Cx46 and Cx50 into gap junctions.

The ultimate C-terminal amino acids of Cx50, Cx46, and Cx43 constitute canonical PDZ-binding domains (Songyang et al., 1997), which have been shown to direct connexin binding to ZO-1 in vitro (Nielsen et al., 2003; Giepmans and Moolenaar, 1998; Toyofuku et al., 1998). Furthermore, HeLa cells express ZO-1 abundantly (Li et al., 2004b). If direct interactions with ZO-1 influence connexin assembly, trafficking, or gating, there should be significant overlap in their distribution. Indeed, double-label immunofluorescence in Cx50-transfected HeLa cells revealed substantial association between ZO-1 and Cx50 (Figure 4, A–C). Plaque-associated Cx50 often labeled for ZO-1, whereas intracellular Cx50 was generally not associated with ZO-1. Some of the ZO-1 signal at cell–cell interfaces, likely corresponding to adherens junctions (Itoh et al., 1993), did not colocalize with Cx50.

If ZO-1 interaction was required for the assembly of junctional plaques by Cx50 and Cx46 in HeLa cells, then experimental reduction of ZO-1 expression should prevent plaque formation. To accomplish this, we treated HeLa cultures with siRNA oligonucleotides corresponding to different nonoverlapping sequences in human ZO-1 or with a scrambled control siRNA and used Western blotting to assess ZO-1 protein levels (Figure 4D). As a control for lane loading, actin levels were also assessed. Although the control siRNA did not affect the levels of ZO-1 (Figure 4D, lane 1), each of the three experimental anti–human ZO-1 siRNAs effectively reduced its expression (Figure 4D, lanes 2–4). Similarly, ZO-1 was generally undetectable by immunofluorescence localization (Figure 4E). The micrograph in Figure 4E was chosen because it contained a cluster of cells that escaped siRNA knockdown (Figure 4E, boxed area) that provided a useful positive control for junctional plaque assembly. Cx50 was unable to form junctional maculae when expressed in ZO-1–depleted cultures (Figure 4F) except in those rare areas where ZO-1 expression was retained (Figure 4, E–G). As expected, junctional transfer of neurobiotin in ZO-1–depleted, Cx50-transfected cells was not observed (Figure 4H).
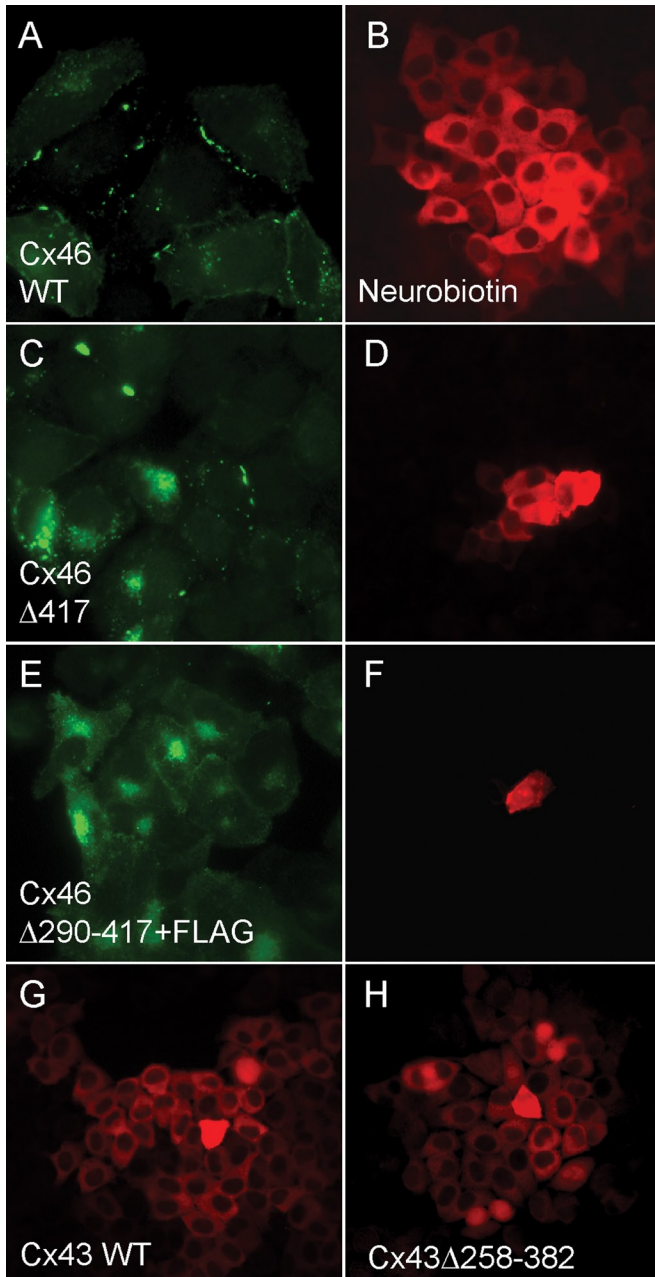
Even though the effects of three different anti–human ZO-1 siRNAs were similar, it was still possible that off-target effects of

FIGURE 2: Assembly and function of Cx46 but not Cx43 is dependent on a C-terminal domain. (A, B) Wild-type Cx46, like Cx50, produced strong macular staining in HeLa cells and robust neurobiotin transfer. (C, D) Deletion of its ultimate C-terminal residue (Cx46Δ417) resulted in a major reduction but not complete loss of macular localization and a complementary reduction of dye transfer. (E, F) FLAG-tagged Cx46 truncated at residue 290 neither formed immunofluorescent puncta nor induced coupling in HeLa cells. (G, H) Wild-type Cx43 expression induced robust dye coupling, which was not affected by severe C-terminal truncation at residue 258.

the siRNAs could account for the changes in connexin behavior. To eliminate this possibility, we restored ZO-1 expression to depleted cells by transfection with mouse ZO-1, which was not affected by the siRNAs designed against human ZO-1 (Figure 4I). Mouse ZO-1 transfection fully restored both plaque formation and dye transfer to siRNA-treated HeLa cells expressing Cx50 (Figure 4, J and K).
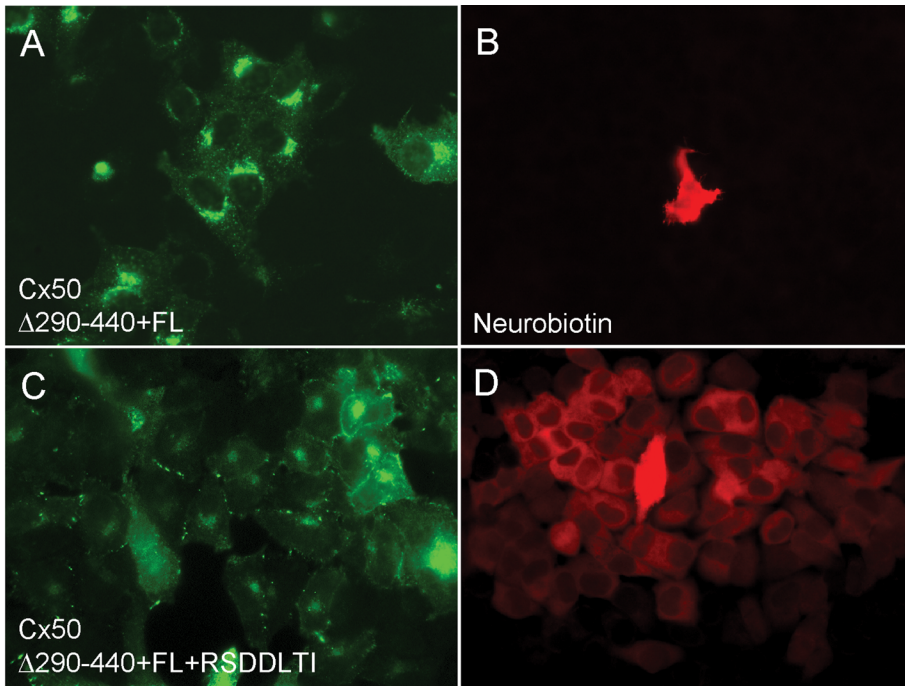
Because lens fibers bear little resemblance to HeLa cells, it remained possible that Cx50 might not exhibit a dependence on its PDZ domain–binding motif for normal function in vivo. Therefore we generated a mouse line in which the Cx50-coding region was replaced with Cx50Δ440, using homologous recombination. The strategy is illustrated in Figure 5 and entails relatively little alteration of the native locus. After cre transfection to remove the neo selection cassette, recombinants retain only ~70 exogenous bases, constituting a loxP site and linker sequences, within the intron upstream of the sole coding exon. To control for possible effects of this exogenous sequence, we also isolated partial recombinants with homologous integration of the neo cassette but not the mutated coding sequences. Animals were produced from both full and partial recombinant embryonic stem (ES) cell lines, and for each, interbreeding of heterozygous parents resulted in offspring with a Mendelian ratio of genotypes.

The overall size of homozygous knock-in, WT littermate control and partially recombinant control animals were similar. However, Cx50Δ440 knock-in lenses were significantly smaller than either type of control lens (Figure 6A). Dissected P28 knock-in lenses weighed 48% less than controls (N = 12; $p < 10^{-23}$, Student's unpaired t test), and a difference in size was evident from at least P6, the earliest time point examined. Knock-in lenses also developed nuclear cataracts consisting of a fine particulate precipitate, which were not observed in controls. Thus the Cx50Δ440 knock-in and the Cx50 knockout (White *et al.*, 1998; Rong *et al.*, 2002) display similar if not identical gross phenotypes, indicating that the Cx50 PDZ-binding motif provides a critical function in vivo.

The distribution of Cx50Δ440 in P12 knock-in lenses and WT Cx50 in littermate control lenses was compared using double-label immunofluorescence (Figure 6, B–J). Cx50Δ440 in the knock-in was evident only in the most superficial cortical fibers (Figure 6, B and D), whereas WT Cx50 in the control was detected in all cortical and some nuclear fibers (Figure 6, G and H). In addition, whereas the signal from WT Cx50 consisted of small puncta evenly distributed along the length of the fibers, Cx50Δ440 accumulated into large, unevenly distributed linear or irregularly shaped patches. Furthermore, higher-than-normal intracellular accumulations of Cx50Δ440 were evident in the anterior epithelium (Figure 6B, arrow) and in newly differentiating fibers (Figure 6I) of the knock-in bow region (compare to control in Figure 6, G and J), consistent with impaired assembly of gap junctions. Cx46 was also abnormally distributed in superficial cortical fibers and anterior epithelium of the knock-in, where it extensively colocalized with Cx50Δ440 (compare Figure 6, C and D, to Figure 6, F and H). However, in more mature fibers, where Cx50Δ440 signal was not detected, Cx46 was arranged in typical plaques.

DISCUSSION

We showed that Cx50 requires ZO-1 in order to assemble junctional plaques and form active intercellular channels in HeLa cells. In addition, a seven–amino acid region containing a PDZ domain–binding motif was necessary for normal trafficking and intercellular channel formation and was sufficient to confer normal behavior on highly truncated versions of Cx50. Our data do not demonstrate that direct binding of ZO-1 to Cx50 occurs, only that ZO-1 is a required partner in the process of forming an active intercellular channel. However, it has been conclusively established that ZO-1 is colocalized and physically associated with Cx50 in vivo and can directly bind Cx50 in vitro (Nielsen *et al.*, 2003; Puller *et al.*, 2009). Thus it is likely that the assembly of Cx50 into junctional plaques involves direct binding between the

FIGURE 3: Seven C-terminal amino acids constituting a PDZ-binding motif are sufficient to confer normal assembly and function on severely truncated Cx50. (A–D) Although FLAG-tagged Cx50 truncated at residue 290 (Cx50Δ290-440+FL) exhibited neither macular localization (A, N) nor conferred dye coupling (B, N), the addition of the ultimate seven amino acids (Cx50Δ290-440+FL+RSDDLTI) was sufficient to restore normal behavior (C, D, O). (E–M) More than seven residues did not increase the level of coupling above WT, while fewer than seven residues did not restore coupling at all. (P, Q) Fusion of RSDDTLI to Cx50 truncated at residue 245 restored WT levels of plaques and dye coupling. (R) Coexpression of Cx50Δ290-440 with a full-length, soluble C-terminal fragment did not restore function. Thus, unlike Cx43, the efficient assembly of Cx50 into gap junctions requires a PDZ-binding motif at its ultimate C-terminus. E, extracellular domain; FL, FLAG tag; IM, intracellular membranes; M, membrane domain; ND, not determined.

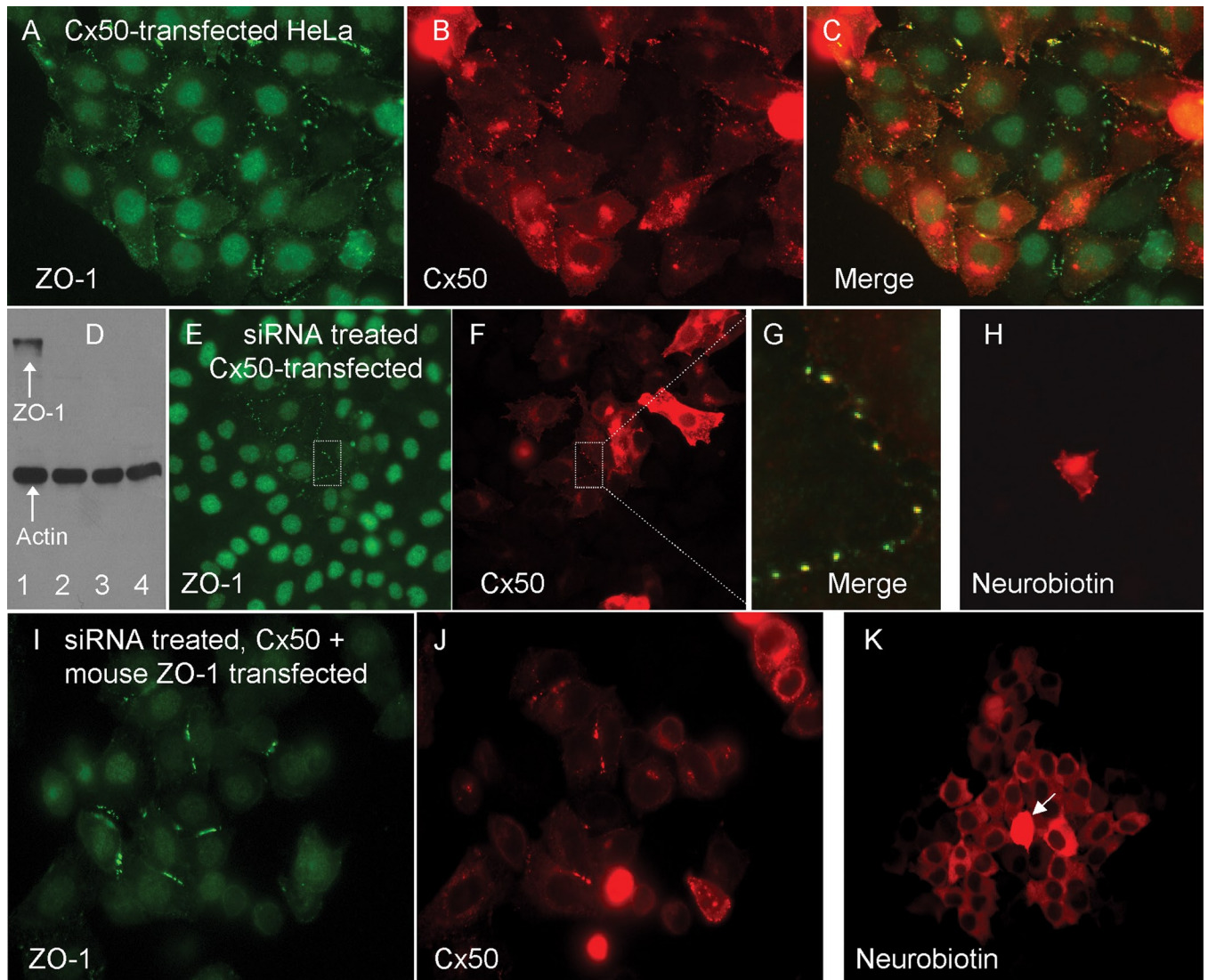| Cx50 C-terminus	Cells coupled	Distribution
E 290+40	46.2±8.5	ND
F 290+21	40.4±7.8	ND
G 290+12	44.6±6.8	ND
H 290+9	47.3±9.5	ND
I 290+8	42.4±7.8	ND
J 290+7	43.6±8.1	ND
K 290+6	0.09±0.3	ND
L 290+5	0.08±0.2	ND
M 290+4	0.09±0.3	ND
N 290+FL	0.09±0.4	IM
O 290+FL+7	42.4±7.8	Plaques
P 245+FL	2.7±2.3	Sparse Plaques
Q 245+FL+7	48.9±9.1	Plaques

1999; Xu et al., 2002; Derosa et al., 2006). However, where measured, the truncation induced only ~10–15% as much conductance as WT. Thus our results are qualitatively similar, in that truncation severely compromised the ability of Cx50 to form gap junctions. The quantitative difference could reflect differences in the expression system, which in our case used a HeLa line specifically selected for the absence of endogenous connexin expression and communication (Magnotti et al., 2011). Consistent with this notion, expression of ovine Cx50Δ290-440 in HeLa cells did not produce significant conductance (Eckert, 2002). It is conceivable that Xenopus oocytes and N2A cells provide alternative assembly mechanisms that partially mask the effect of ZO-1 binding.

Our data are in apparent contradiction with an earlier study in which Cx50 lacking the C-terminal isoleucine was reported to assemble plaque-like structures at HEK293 cell–cell interfaces (Nielsen et al., 2003). In our hands, expression of this Cx50 mutant in HeLa cells resulted in immunofluorescence signal at intracellular locations and occasionally at or near the cell surface (Figure 1B, arrow). The surface staining included cell–cell interfaces and thus might correspond to the structures reported in HEK cells. However, the mutant was never observed in small, well-defined macula at cell–cell interfaces as was WT Cx50, and it did not induce cell–cell communication in HeLa cells. Thus one possibility is that the structures reported by Nielsen et al. (2003) are not actually gap junctional plaques. Alternatively, because HEK cells express endogenous Cx43 abundantly, the staining reported by Nielsen et al. (2003) might represent Cx43-containing gap junctions that were able to incorporate mutant Cx50.

Because it is unlikely that neither HeLa cells nor any other in vitro system accurately models lens fibers, we tested the generality of our findings by constructing a knock-in mouse line expressing Cx50 with a PDZ-binding motif mutation. The knock-in phenocopied a Cx50 null line we characterized previously (White et al., 1998) and displayed highly abnormal connexin distribution, consistent with our hypothesis of grossly impaired gap junction assembly. Cx46 distribution is also abnormal in the cortical fibers of the knock-in, which likely reflects the well-documented heteromeric interaction between these connexins (Jiang and Goodenough, 1996; Ebihara et al., 1999; Hopperstad et al., 2000). Overlap between Cx46 and Cx50Δ440 in the knock-in is extensive but not complete, and Cx46 in the deeper fibers, possibly that which escapes oligomerization with Cx50, forms plaques that are normal in appearance. The presence of large aggregations of connexin in what may be cortical fiber plasma membrane leaves open the possibility that some Cx50 gap junction assembly might occur. However, the simplest interpretation of in vitro

connexin and ZO-1. In contrast, whereas Cx43 exhibits a similar PDZ-binding motif, ZO-1 was not required for its assembly into a gap junction. Finally, we showed that knock-in mice expressing Cx50 lacking its ultimate C-terminal residue display a phenotype similar to Cx50-null mice and that this mutant connexin fails to assemble typical junctional plaques in vivo. This study provides the first example of a connexin type–specific requirement for a connexin-interacting protein in gap junction assembly. Together with other studies, our data suggest the existence of multiple mechanisms for targeting connexins to junctional plaques.

Although we found no evidence that Cx50 truncated at residue 290 formed intercellular channels, earlier studies reported that this truncation induced junctional communication in Xenopus oocyte pairs and N2A cells (Lin et al., 1998; Stergiopoulos et al.,

FIGURE 4: The PDZ-domain scaffolding protein ZO-1 is required for normal assembly and function of Cx50. (A–C) Double-label immunofluorescence for Cx50 (red) and ZO-1 (green) in Cx50-transfected HeLa cells. Nuclear signal is a nonspecific background staining. Cx50 and ZO-1 were often closely associated. (D) Western blot for ZO-1 and actin in HeLa cells treated with different siRNAs. Three nonoverlapping anti–ZO-1 siRNAs were equally effective at reducing steady-state protein levels (lanes 2–4), whereas a scrambled control (lane 1) had little effect. Actin served as a loading control. (E–G) Double immunofluorescence labeling for Cx50 and ZO-1 in siRNA-treated cells. ZO-1 staining was greatly reduced (compare E and A), and Cx50 puncta were generally not observed, although intracellular Cx50 signal was abundant (compare F and B). The boxed area in E and F (shown at higher magnification in G) shows an area where ZO-1 expression was retained. Note that Cx50 puncta are observed only in this region. (H) Neurobiotin transfer (red) was not observed in ZO-1–depleted, Cx50-transfected cells. (I–K) Mouse ZO-1 transfection fully restored both plaque formation (J) and dye transfer (K) to siRNA-treated HeLa cells expressing Cx50. Arrow indicates the injected cell.

and in vivo data taken together is that gap junctions containing Cx50 do not form.

The difference in ZO-1 dependence for intercellular trafficking of Cx50 and Cx43 is surprising, given the high degree of identity in their C-terminal amino acids, which exhibit canonical class II PDZ domain–binding motifs (Lee and Zheng, 2010), and the fact that all three have been shown to directly bind ZO-1 (Giepmans and Moolenaar, 1998; Toyofuku et al., 1998; Nielsen et al., 2003). One explanation consistent with the literature would be the presence of alternative, potentially connexin-specific, mechanisms for trafficking and/or assembly. For example, both Cx43 and Cx32 are expressed in thyroid epithelia, but Cx43 is targeted to the area of the tight junctions, whereas Cx32 (which does not bind ZO-1) tar-

gets independently to the lateral cell surfaces (Guerrier et al., 1995). Furthermore, it has been shown, using transfected mammalian cell cultures, that Cx43 and Cx32 trafficking is highly sensitive to brefeldin A treatment but that of Cx26 is not (Martin et al., 2001).

More is known about the trafficking and assembly of Cx43 than about any other connexin. Cx43-based gap junction formation depends on the assembly of adherens junctions (Keane et al., 1988; Meyer et al., 1992; Frenzel and Johnson, 1996) and requires the expression of the adherens junction protein N-cadherin both in vitro and in vivo (Wei et al., 2005). More recently, it has been shown that Cx43 hemichannels can be targeted directly from the trans-Golgi network to adherens junctions through a microtubule-dependent
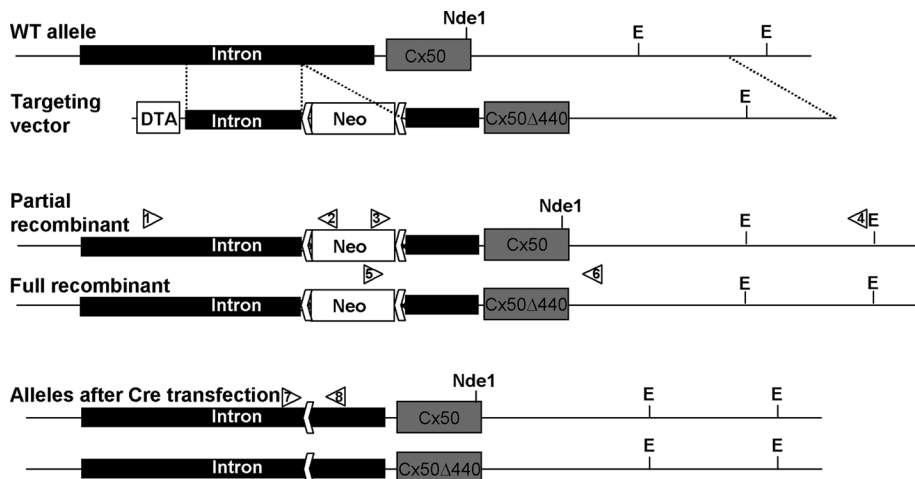
FIGURE 5: Construction of the Cx50Δ440 knock-in mouse. The Cx50 coding sequence is contained in a single exon following a 5.5-kb intron. The targeting vector added a floxed PGK–neomycin resistance cassette inside the intron and a PGK–diphtheria toxin A chain cassette outside the 5′ homology and contained a three-base deletion in the coding sequence deleting the ultimate C-terminal residue. Initial screening for homologous recombinants used PCR amplification with primers outside the 5′ homology arm (1) and in the neo cassette (2). A secondary screen verified 3′ structure using primers in the neo cassette (3) and outside the 3′ homology arm (4). Because the Cx50Δ440 mutation eliminated an *Nde*1 site, the presence of the mutation was confirmed by restriction digestion. In addition to fully recombined clones, several were identified with partial recombination, resulting in homologous integration of the neo cassette but leaving the native coding sequence, providing an ideal negative control. Recombinant ES clones were then transfected with *cre* recombinase and screened for neo excision using primers P7 and P8.

pathway involving the microtubule plus end–tracking protein EB1, its interacting protein p150, and the adherens junction protein β-catenin (Shaw *et al.*, 2007). At the adherens junction, Cx43 becomes complexed with N-cadherin, α- and β-catenins, and p120 (Wei *et al.*, 2005), after which interactions between Cx43 and ZO-1 that limit the size of growing gap junctions may occur (Hunter *et al.*, 2005). A microtubule-based mechanism may also be used by Cx26 (Shaw *et al.*, 2007), although Cx26 is less dependent on it than is Cx43 (Thomas *et al.*, 2001). The influence of microtubule-based mechanisms on the trafficking of other connexins has not been determined, but our results indicate that Cx50 and Cx46 trafficking involves a novel pathway not used by Cx43.

A significant difference in the interactions of Cx43 and Cx50 with caveolin and lipid microdomains suggests a possible explanation for their difference in ZO-1 dependence. Cx43 binds caveolin-1, -2, and -3 (Schubert *et al.*, 2002; Langlois *et al.*, 2008; Liu *et al.*, 2010) and becomes associated with lipid rafts, whereas Cx50 does not coprecipitate with caveolin-1 and is excluded from rafts. Furthermore, truncation of Cx43 at residue 257 does not affect caveolin binding or targeting to rafts (Schubert *et al.*, 2002), indicating that those behaviors are independent of ZO-1. Truncation at residue 244 eliminates both caveolin binding and raft association (Langlois *et al.*, 2008). Together, these data are consistent with a model in which caveolin binding near the start of the connexin C-terminal cytosolic domain could be part of a separate trafficking pathway available to Cx43 but not Cx50. In contrast to Cx50, Cx46 might use both ZO-1 and caveolin-dependent pathways for intercellular trafficking since removal of its terminal isoleucine reduced but did not eliminate its ability to form functional channels. Finally, it is noteworthy that although Cx50Δ290-440 neither formed detectable plaques nor induced detectable cell–cell coupling, a deeper truncation (Cx50Δ245-440) induced a modest level of coupling. One interpre-

tation would be the existence of a domain between residues 245 and 290 that specifically inhibits Cx50 trafficking and whose inhibition is relieved by ZO-1 binding at another site.

In summary, we showed that the PDZ domain–binding motif of Cx50 is required for assembly into gap junctions in communication-incompetent HeLa cells, as well as for normal function in vivo. Furthermore, unlike Cx43, ZO-1 is critical for junctional assembly of Cx50 in HeLa cells. It remains to be demonstrated whether a PDZ-binding motif and ZO-1 are required for junction assembly of other connexins with binding motifs, such as Cx31.9, Cx45, and Cx47, and whether the molecular mechanisms underlying Cx43 trafficking are used by Cx50.

MATERIALS AND METHODS
Connexin expression constructs and HeLa cell transfections

PCR amplification was used to produce DNAs encoding full-length and truncated versions of mouse Cx50 (White *et al.*, 1992), rat Cx46 (Paul *et al.*, 1991), and mouse Cx43 (Beyer *et al.*, 1987). Where fusions to FLAG tags and/or domains from distal portions of connexin C-termini were desired, sequences encoding those features were incorporated into the 3′ oligonucleotides priming the amplifications. PCR products were then subcloned into the *Eco*RI site of pIRES2-Venus or Cerulean (Clontech, Mountain View, CA) and fully sequenced to verify the mutations. The HeLa cell subclone described in Magnotti *et al.* (2011) was used for transient expression in this study because it was completely communication negative under the conditions of our assay. Cells were cultured in high-glucose DMEM (Invitrogen, Carlsbad, CA) with sodium pyruvate containing 10% fetal bovine serum (FBS; HyClone, Logan, UT) and 1% penicillin/streptomycin (Invitrogen). HeLa cells were transfected with DNA plasmids using Lipofectamine (Invitrogen) according to the manufacturer's directions. For knockdown of endogenous ZO-1, 25-mer RNA duplexes were synthesized (Stealth RNAi; Invitrogen) corresponding to bases 940–965, 2458–2483. and 3211–3236 in accession sequence NM_175610. These sequences were chosen to suppress expression of human but not mouse ZO-1. A scrambled control for 940–965 (5′-GCCGGAGAUAGGAGUAC-GAUAGAGA) was also prepared. HeLa cells were transfected with RNAi duplexes using Lipofectamine 2000 (Invitrogen) according to the manufacturer's directions and incubated for 40 h to allow turnover and elimination of preexisting ZO-1 protein.

Dye injection

Three days prior to the dye transfer assay, cells were plated on 35-mm glass-bottom Fluorodishes (World Precision Instruments, Sarasota, FL) and incubated in culture media as described earlier supplemented with 400 ng/μl unlabeled avidin (Sigma-Aldrich, St. Louis, MO) to eliminate the background signal from endogenous biotin-containing compounds (Magnotti *et al.*, 2011). Cells were grown to confluence and transferred to a 4-(2-hydroxyethyl)-1-piperazineethanesulfonic acid (HEPES)–buffered solution containing 150 mM NaCl, 5 mM KCl, 2 mM CaCl₂, 1 mM
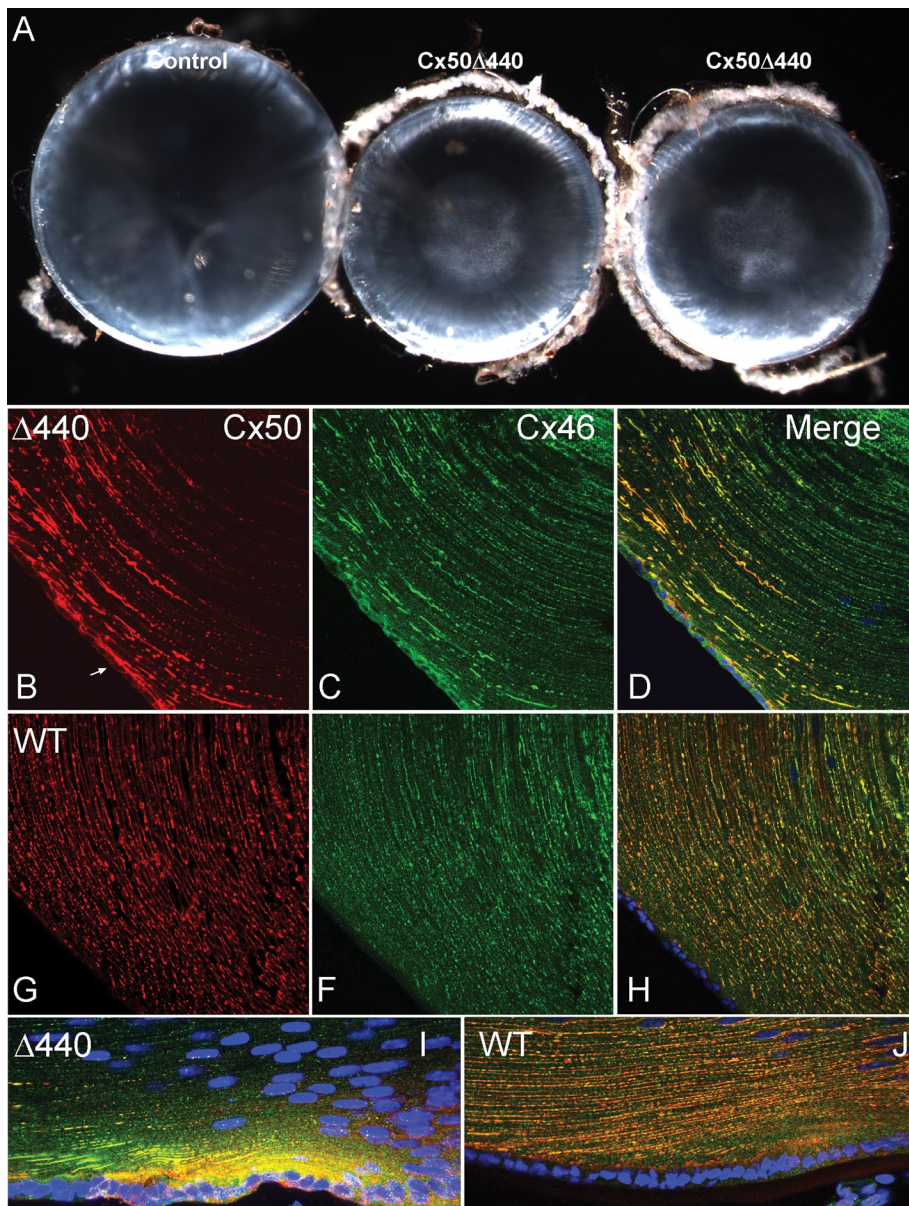
FIGURE 6: Cx50Δ440 homozygote lenses are small, with nuclear cataracts, and display abnormal connexin distribution. (A) A comparison of Cx50Δ440 knock-in lenses (middle, right) and littermate controls (left) at P28. Knock-in lenses were smaller and developed nuclear cataracts, similar to Cx50-null mouse lines (White et al., 1998; Rong et al., 2002). (B–J) An immunofluorescence comparison of connexin distribution in P12 knock-in and littermate control lenses. (B) Cx50Δ440 was only evident in superficial cortical fibers and accumulated in large linear or irregular patches. Intracellular signal in epithelium (arrow) is higher than in control. (C) Cx46 distribution in the knock-in was abnormal in anterior epithelium and superficial fibers, but deeper fibers displayed typical plaques. (G, F, H) Cx50 and Cx46 were evenly distributed in small puncta in all fibers of the control. (I) High levels of intracellular Cx50Δ440 were evident in bow region fibers of the knock-in. (J) Intracellular connexin is not obvious in control bow region.

alternating currents of −1 and +1 nA at 200 ms each for a total of 1 min. Ten injections were performed per dish, and the total time of the experiment never exceeded 15 min. A minimum of three dishes was used for each cell type, for a total of 30 injections. For neurobiotin detection, cells were fixed in 4% paraformaldehyde for 15 min, blocked with 1% fish skin gelatin in phosphate-buffered saline (PBS) containing 0.1% Tween-20 for 30 min, and incubated in tetramethylrhodamine-conjugated NeutrAvidin (1:1000; Invitrogen) for 1 h at room temperature.

Immunostaining

Cells were grown on coverslips, fixed with 4% paraformaldehyde for 15 min at room temperature, blocked with 10% fetal bovine serum in PBS containing 0.2% Tween-20, and incubated for 1 h at room temperature in appropriate combinations of the following primary antibodies: goat anti-Cx50 (1:500; SC-20876; Santa Cruz Biotechnology, Santa Cruz, CA), rabbit anti-Cx46 (1:500; 70-0384; Invitrogen), rabbit anti-Cx43 (1:10,000; C-6219; Sigma-Aldrich), rabbit anti–human ZO-1 (1:500; 40-2300; Invitrogen), mouse anti–human ZO-1 (1:100; 33-9100; Invitrogen), or mouse anti–FLAG M2 (1:1000; F1804; Sigma-Aldrich). After incubation with primary antibodies, cells were washed and incubated with appropriate Alexa 488– or 568–labeled secondary antibodies (1:500; Invitrogen) in blocking solution for 1 h at room temperature, washed, and mounted using VectaShield (Vector Laboratories). Micrographs were acquired using a Nikon E800 microscope (Nikon, Melville, NY) equipped with epifluorescence optics and Spot RT3 digital camera (Diagnostic Instruments, Sterling Heights, MI). Distribution of transfected connexin was assessed in at least 30 randomly chosen fields photographed at 60× magnification, obtained from at least three independent transfections. Junction-like structures were never observed for any Cx50 mutant. In contrast, junction-like structures were readily observed in every field when WT connexins were transfected.

MgCl$_2$, and 10 mM D-glucose, pH 7.4, immediately prior to dye transfer assay. The nonfluorescent tracer neurobiotin (molecular weight [MW], 287; +1 charge; Vector Laboratories, Burlingame, CA) was dissolved at 10% along with 3% dextran–Cascade Blue (MW = 10,000; Invitrogen) in a HEPES-buffered solution of 140 mM KCl, 2 mM MgCl$_2$, 6 mM ethylene glycol tetraacetic acid, and 5 mM CsCl. Pipettes were backfilled with tracer solution, and iontophoretic injection was carried out by applying

Construction of the knock-in mouse line

WT Cx50 was replaced by Cx50Δ440, using the same general strategy previously used (White, 2002); a floxed phosphoglycerate kinase 1 (PGK)–neomycin resistance cassette was placed within an intron upstream of the Cx50-coding region to provide positive selection, and a PGK–diphtheria toxin A chain cassette was placed outside the 5′ homology region to provide negative selection. The 3′ homology arm, which contained ~500 base pairs of intronic sequence, the

complete coding region, and 5.5 kb of 3' flanking genomic sequence, was amplified from J1 ES cell genomic DNA using primers containing Sal1 (ATA TAT **GTC GAC** AAC AGG ACT AAG ATA AAC GAA ATG) and Sma1 sites (TTT TTT **CCC GGG** ACC GGG AAC TCC AAA AGA ATA A), subcloned into the targeting vector pDTA (gift of Frank Gertler), and completely sequenced. A 1.5-kb fragment encompassing the site for the desired mutation, as well as unique flanking SnaB1 and BsaB1 restriction sites, was amplified from the 3' homology arm using primers containing Xho1 (TTT TTT **CTC GAG** GAT GAC AAT CGG CCC TTG AGC) and Sma1 (TTT TTT **CCC GGG** TAC GTA TAC TTG ATA TTT TTT TC) sites and subcloned into pIRES2 (Clontech) for mutagenesis. The Cx50Δ440 mutation was created using the QuikChange II Site-Directed Mutagenesis Kit (Stratagene, Santa Clara, CA), sequenced, and released by SnaB1/BsaB1 digestion for transfer back into pDTA containing the WT 3' arm. The 5' homology arm, containing 1.9 kb of intron sequence, was amplified from ES cell DNA with primers containing SacII (ATA TAT **CCG CGG** CCA GTT GGG CTC ATC TTA CCT) and Not1 (TTT TTT **GCG GCC GC**G CAT AGC CAA TTC CCG CAC AC) sites, subcloned into pDTA + 3' arm, and sequenced, completing the targeting construct.

J1 ES cells were electroporated as previously described, and 276 neomycin-resistant clones were selected. Homologous recombinants were initially identified using PCR amplification with primers outside the 5' homology arm (P1) and in the neo cassette (P2). A secondary screen to verify 3' structure was conducted using primers in the neo cassette (P3) and outside the 3z homology arm (P4). Because the Cx50Δ440 mutation eliminated an Nde1 site, the presence of the mutation was confirmed by restriction digestion. A primer within the neo cassette (P5) and a primer 270 base pairs downstream of the Cx50 stop codon (P6) were used to amplify a 3.2-kb segment of genomic DNA, which was subjected to Nde1digestion, releasing a 271–base pair fragment from the WT but not the mutant allele. Seven fully recombined clones were identified, as well as two with a partial recombination resulting in homologous integration of the neo cassette but leaving the native coding sequence, providing an ideal negative control.

To remove the selection cassette, ES cell clones with good karyotypes were transfected with cre recombinase. A total of 132 fully recombined and 112 partially recombined clones were screened by PCR for neo excision using primers P7 and P8, which produced a 2.2-kb band before neo excision, 477 base pairs after excision, and a 401–base pair band from the WT allele. Fifteen correctly recombined and five partially recombined clones were identified. Lines with good karyotypes were injected into C57/BL6 blastocysts, and highly chimeric pups were crossed with WT C57/BL6 to obtain Cx50Δ440 heterozygotes:

P1: CCC TGG GCC ATG ACT GTG TAT C
P2: CCA AGC GGC CGG AGA ACC TG
P3: GGC GGC GAA TGG GCT GAC C
P4: ATG GGG GAG GGG CTG AGT AAG TGG
P5: GGG CGC CCG GTT CTT TTT GTC
P6: AGC CCC CAT CCC CAC CTT CCT AAC
P7: GAC CAT CTG TTT AGC CTC AA
P8: GAA TTT AAA TCA AGA CCA TAC G

REFERENCES

Beyer EC, Paul DL, Goodenough DA (1987). Connexin43: a protein from rat heart homologous to a gap junction protein from liver. J Cell Biol 105, 2621–2629.

Brizzard BL, Chubet RG, Vizard DL (1994). Immunoaffinity purification of FLAG epitope-tagged bacterial alkaline phosphatase using a novel monoclonal antibody and peptide elution. Biotechniques 16, 730–735.

Derosa AM, Mui R, Srinivas M, White TW (2006). Functional characterization of a naturally occurring cx50 truncation. Invest Ophthalmol Vis Sci 47, 4474–4481.

Ebihara L, Xu X, Oberti C, Beyer EC, Berthoud VM (1999). Co-expression of lens fiber connexins modifies hemi-gap-junctional channel behavior. Biophys J 76, 198–206.

Eckert R (2002). pH gating of lens fibre connexins. Pflugers Arch 443, 843–851.

Elfgang C, Eckert R, Lichtenberg-Fraté H, Butterweck A, Traub O, Klein RA, Hülser DF, Willecke K (1995). Specific permeability and selective formation of gap junction channels in connexin-transfected HeLa cells. J Cell Biol 129, 805–817.

Flores CE, Li X, Bennett MV, Nagy JI, Pereda AE (2008). Interaction between connexin35 and zonula occludens-1 and its potential role in the regulation of electrical synapses. Proc Natl Acad Sci USA 105, 12545–12550.

Frenzel EM, Johnson RG (1996). Gap junction formation between cultured embryonic lens cells is inhibited by antibody to N-cadherin. Dev Biol 179, 1–16.

Giepmans BN, Moolenaar WH (1998). The gap junction protein connexin43 interacts with the second PDZ domain of the zona occludens-1 protein. Curr Biol 8, 931–934.

Goodenough DA, Paul DL (2009). Gap junctions. Cold Spring Harbor Perspect Biol 1:a002576.

Guerrier A, Fonlupt P, Morand I, Rabilloud R, Audebet C, Krutovskikh V, Gros D, Rousset B, Munari-Silem Y (1995). Gap junctions and cell polarity: connexin32 and connexin43 expressed in polarized thyroid epithelial cells assemble into separate gap junctions, which are located in distinct regions of the lateral plasma membrane domain. J Cell Sci 108, 2609–2617.

Helbig I, Sammler E, Eliava M, Bolshakov AP, Rozov A, Bruzzone R, Monyer H, Hormuzdi SG (2010). In vivo evidence for the involvement of the carboxy terminal domain in assembling connexin 36 at the electrical synapse. Mol Cell Neurosci.

Hopperstad MG, Srinivas M, Spray DC (2000). Properties of gap junction channels formed by Cx46 alone and in combination with Cx50. Biophys J 79, 1954–1966.

Hunter AW, Barker RJ, Zhu C, Gourdie RG (2005). ZO-1 alters connexin43 gap junction size and organization by influencing channel accretion. Mol Biol Cell 16, 5686–5698.

Hunter AW, Gourdie RG (2008). The second PDZ domain of zonula occludens-1 is dispensable for targeting to connexin 43 gap junctions. Cell Commun Adhes 15, 55–63.

Itoh M, Nagafuchi A, Yonemura S, Kitani-Yasuda T, Tsukita S, Tsukita SH (1993). The 220-kD protein colocalizing with cadherins in non-epithelial cells is identical to ZO-1, a tight junction-associated protein in epithelial cells: cDNA cloning and immunoelectron microscopy. J Cell Biol 121, 491–502.

Jiang JX, Goodenough DA (1996). Heteromeric connexons in lens gap junction channels. Proc Natl Acad Sci USA 93, 1287–1291.

Kausalya PJ, Reichert M, Hunziker W (2001). Connexin45 directly binds to ZO-1 and localizes to the tight junction region in epithelial MDCK cells. FEBS Lett 505, 92–96.

Keane RW, Mehta PP, Rose B, Honig LS, Loewenstein WR, Rutishauser U (1988). Neural differentiation, NCAM-mediated adhesion, and gap junctional communication in neuroectoderm. A study in vitro. J Cell Biol 106, 1307–1319.

Koval M (2006). Pathways and control of connexin oligomerization. Trends Cell Biol 16, 159–166.

Laing JG, Manley-Markowski RN, Koval M, Civitelli R, Steinberg TH (2001). Connexin45 interacts with zonula occludens-1 and connexin43 in osteoblastic cells. J Biol Chem 276, 23051–23055.

Langlois S, Cowan KN, Shao Q, Cowan BJ, Laird DW (2008). Caveolin-1 and -2 interact with connexin43 and regulate gap junctional intercellular communication in keratinocytes. Mol Biol Cell 19, 912–928.

Lee HJ, Zheng JJ (2010). PDZ domains and their binding partners: structure, specificity, and modification. Cell Commun Signal 8, 8.

Li X, Ionescu AV, Lynn BD, Lu S, Kamasawa N, Morita M, Davidson KG, Yasumura T, Rash JE, Nagy JI (2004a). Connexin47, connexin29 and connexin32 co-expression in oligodendrocytes and cx47 association

with zonula occludens-1 (ZO-1) in mouse brain. Neuroscience 126, 611–630.

Li X, Lu S, Nagy JI (2009). Direct association of connexin36 with zonula occludens-2 and zonula occludens-3. Neurochem Int 54, 393–402.

Li X, Olson C, Lu S, Kamasawa N, Yasumura T, Rash JE, Nagy JI (2004b). Neuronal connexin36 association with zonula occludens-1 protein (ZO-1) in mouse brain and interaction with the first PDZ domain of ZO-1. Eur J Neurosci 19, 2132–2146.

Lin JS, Eckert R, Kistler J, Donaldson P (1998). Spatial differences in gap junction gating in the lens are a consequence of connexin cleavage. Eur J Cell Biol 76, 246–250.

Lin JS, Fitzgerald S, Dong YM, Knight C, Donaldson P, Kistler J (1997). Processing of the gap junction protein connexin50 in the ocular lens is accomplished by calpain. Eur J Cell Biol 73, 141–149.

Liu L, Li Y, Lin J, Liang Q, Sheng X, Wu J, Huang R, Liu S, Li Y (2010). Connexin43 interacts with caveolin-3 in the heart. Mol Biol Rep 37, 1685–1691.

Maass K et al. (2004). Defective epidermal barrier in neonatal mice lacking the c-terminal region of connexin43. Mol Biol Cell 15, 4597–4608.

Magnotti LM, Goodenough DA, Paul DL (2011). Functional heterotypic interactions between astrocyte and oligodendrocyte connexins. Glia 59, 26–34.

Manthey D, Banach K, Desplantez T, Lee CG, Kozak CA, Traub O, Weingart R, Willecke K (2001). Intracellular domains of mouse connexin26 and -30 affect diffusional and electrical properties of gap junction channels. J Membr Biol 181, 137–148.

Martin PE, Blundell G, Ahmad S, Errington RJ, Evans WH (2001). Multiple pathways in the trafficking and assembly of connexin 26, 32 and 43 into gap junction intercellular communication channels. J Cell Sci 114, 3845–3855.

Meyer RA, Laird DW, Revel JP, Johnson RG (1992). Inhibition of gap junction and adherens junction assembly by connexin and A-CAM antibodies. J Cell Biol 119, 179–189.

Morley GE, Taffet SM, Delmar M (1996). Intramolecular interactions mediate pH regulation of connexin43 channels. Biophys J 70, 1294–1302.

Musil LS, Cunningham BA, Edelman GM, Goodenough DA (1990). Differential phosphorylation of the gap junction protein connexin43 in junctional communication-competent and deficient cell lines. J Cell Biol 111, 2077–2088.

Nielsen PA, Baruch A, Shestopalov VI, Giepmans BN, Dunia I, Benedetti EL, Kumar NM (2003). Lens connexins α3 (Cx46) and α8 (Cx50) interact with zonula occludens protein-1 (ZO-1). Mol Biol Cell 14, 2470–2481.

Nielsen PA, Beahm DL, Giepmans BN, Baruch A, Hall JE, Kumar NM (2002). Molecular cloning, functional expression, and tissue distribution of a novel human gap junction forming protein, connexin-31.9. J Biol Chem 277, 38272–38283.

Puller C, de Sevilla Muller LP, Janssen-Bienhold U, Haverkamp S (2009). ZO-1 and the spatial organization of gap junctions and glutamate receptors in the outer plexiform layer of the mammalian retina. J Neurosci 29, 6266–6275.

Orthmann-Murphy JL, Freidin M, Fischer E, Scherer SS, Abrams CK (2007). Two distinct heterotypic channels mediate gap junction coupling between astrocyte and oligodendrocyte connexins. J Neurosci 27, 13949–13957.

Paul DL, Ebihara L, Takemoto LJ, Swenson KI, Goodenough DA (1991). Connexin46, a novel lens gap junction protein, induces voltage-gated currents in nonjunctional plasma membrane of Xenopus oocytes. J Cell Biol 115, 1077–1089.

Qu C, Gardner P, Schrijver I (2009). The role of the cytoskeleton in the formation of gap junctions by connexin 30. Exp Cell Res 315, 1683–1692.

Rong P, Wang X, Niesman I, Wu Y, Benedetti LE, Dunia I, Levy E, Gong X (2002). Disruption of Gja8 (alpha8 connexin) in mice leads to microphthalmia associated with retardation of lens growth and lens fiber maturation. Development 129, 167–174.

Schubert AL, Schubert W, Spray DC, Lisanti MP (2002). Connexin family members target to lipid raft domains and interact with caveolin-1. Biochemistry 41, 5754–5764.

Segretain D, Falk MM (2004). Regulation of connexin biosynthesis, assembly, gap junction formation, and removal. Biochim Biophys Acta 1662, 3–21.

Shaw RM, Fay AJ, Puthenveedu MA, von Zastrow M, Jan YN, Jan LY (2007). Microtubule plus-end-tracking proteins target gap junctions directly from the cell interior to adherens junctions. Cell 128, 547–560.

Singh D, Solan JL, Taffet SM, Javier R, Lampe PD (2005). Connexin43 interacts with zona occludens-1 and -2 proteins in a cell cycle stage specific manner. J Biol Chem 280, 30416–30421.

Songyang Z, Fanning AS, Fu C, Xu J, Marfatia SM, Chishti AH, Crompton A, Chan AC, Anderson JM, Cantley LC (1997). Recognition of unique carboxyl-terminal motifs by distinct PDZ domains. Science 275, 73–77.

Stergiopoulos K, Alvarado JL, Mastroianni M, Ek-Vitorin JF, Taffet SM, Delmar M (1999). Hetero-domain interactions as a mechanism for the regulation of connexin channels. Circ Res 84, 1144–1155.

Stevenson BR, Siliciano JD, Mooseker MS, Goodenough DA (1986). Identification of ZO-1: a high molecular weight polypeptide associated with the tight junction (zonula occludens) in a variety of epithelia. J Cell Biol 103, 755–766.

Thomas T, Jordan K, Laird DW (2001). Role of cytoskeletal elements in the recruitment of Cx43-GFP and Cx26- YFP into gap junctions. Cell Adhes Commun 8, 231–236.

Toyofuku T, Yabuki M, Otsu K, Kuzuya T, Hori M, Tada M (1998). Direct association of the gap junction protein connexin-43 with ZO-1 in cardiac myocytes. J Biol Chem 273, 12725–12731.

VanSlyke JK, Naus CC, Musil LS (2009). Conformational maturation and post-ER multisubunit assembly of gap junction proteins. Mol Biol Cell 20, 2451–2463.

Wei CJ, Francis R, Xu X, Lo CW (2005). Connexin43 associated with an N-cadherin-containing multiprotein complex is required for gap junction formation in NIH3T3 cells. J Biol Chem 280, 19925–19936.

White TW (2002). Unique and redundant connexin contributions to lens development. Science 295, 319–320.

White TW, Bruzzone R, Goodenough DA, Paul DL (1992). Mouse Cx50, a functional member of the connexin family of gap junction proteins, is the lens fiber protein MP70. Mol Biol Cell 3, 711–720.

White TW, Bruzzone R, Wolfram S, Paul DL, Goodenough DA (1994). Selective interactions among the multiple connexin proteins expressed in the vertebrate lens: the second extracellular domain is a determinant of compatibility between connexins. J Cell Biol 125, 879–892.

White TW, Goodenough DA, Paul DL (1998). Targeted ablation of connexin50 in mice results in microphthalmia and zonular pulverulent cataracts. J Cell Biol 143, 815–825.

Xu X, Berthoud VM, Beyer EC, Ebihara L (2002). Functional role of the carboxyl terminal domain of human connexin 50 in gap junctional channels. J Membr Biol 186, 101–112.

Zhang JT, Chen MG, Foote CI, Nicholson BJ (1996). Membrane integration of in vitro-translated gap junctional proteins—co- and post-translational mechanisms. Mol Biol Cell 7, 471–482.